Subdiffusive random growth of bacteria

Jialiang Wei[1] and Jie Lin[2,3,*]

[1] *School of Physics, Peking University, Beijing, China*
[2] *Center for Quantitative Biology, Peking University, Beijing, China*
[3] *Peking-Tsinghua Center for Life Sciences, Peking University, Beijing, China*

(Dated: March 19, 2026)

While the regulation of bacterial cell size is widely studied across generations, the stochastic nature of cell volume growth remains elusive within a cell cycle. Here, we investigate the fluctuations of cell volume growth and report a deviation from standard white-noise models: the random growth rate exhibits subdiffusive dynamics. Specifically, the mean square displacement of the growth-rate noise scales as Δt^{α} with an anomalous exponent $\alpha \approx 0.27$. This low exponent implies strong negative temporal correlations in growth rate noise on timescales of minutes, which are significantly faster than those of gene expression dynamics. We attribute this phenomenon to the physical mechanics of the cell wall. By modeling the peptidoglycan network as a complex viscoelastic material with power-law-distributed relaxation times, we successfully recapitulate the observed subdiffusive behavior. Our results suggest that the heterogeneous mechanical constraints of the peptidoglycan network, rather than biological regulatory programs,govern the short-timescale fluctuations of bacterial growth.

Introduction—Understanding how bacteria regulate their size is a fundamental question in quantitative biology [1, 2]. Phenomenological models, such as the "adder" model, have successfully described cell size control at the intergenerational level [3–5]. Regarding the average growth dynamics within a cell cycle, it has been suggested that bacterial cell volumes grow exponentially over time [4–7]. Nevertheless, recent studies on *Escherichia coli* and *Caulobacter crescentus* have suggested that growth is not strictly exponential but exhibits a "superexponential" acceleration toward the end of the cell cycle [8–10]. However, it remains unclear whether the observed growth-rate variations reflect intrinsic biological programs or arise as artifacts of the statistical methods used to analyze stochastic trajectories. What is even more elusive is the stochastic nature of cell volume growth on top of the deterministic growth pattern within a cell cycle, and how a bacterial cell regulates its volume on a shorter time scale than the cell cycle.

In this Letter, we employ a minimal drifted Brownian model as a controlled benchmark to evaluate common statistical frameworks. We demonstrate that conditioning average growth rates on relative age, volume, or elapsed time since cell birth inherently introduces systematic biases that can be mistakenly interpreted as biological signals. After accounting for these artifacts, our analysis of experimental data of *E. coli* confirms a genuine growth-rate acceleration in the second half of the cell cycle, supporting the conclusion of superexponential growth.

More significantly, we investigate the fluctuations of cell volume growth on top of the non-exponential deterministic growth. Strikingly, the random growth rate of cell volume exhibits a subdiffusive fluctuation. If we consider the growth-rate noise as the velocity of an imaginary particle and the logarithmic volume $z \equiv \ln(V/\bar{V}_b)$ as its position, the resulting mean square displacement (MSD) of z scales as $\sigma_z^2(\Delta t) \sim \Delta t^{\alpha}$ with an anomalous exponent $\alpha \approx 0.27$. This subdiffusion implies that the growth-rate noise exhibits negative temporal correlations.

Given that the subdiffusion occurs on a time scale of minutes, much shorter than the time scales of significant changes in protein concentrations, we hypothesize that this phenomenon has a physical origin. Given the fact that the deformation of the cell wall is a prerequisite of cell volume growth, we propose that the subdiffusive random growth of cell volume is a consequence of the complex viscoelastic behavior of the cell wall [11–15]. Specifically, we model the cell wall as a complex viscoelastic material composed of multiple serially connected Voigt elements with power-law-distributed relaxation times. This simple model successfully recapitulates subdiffusive growth behavior, and our results suggest that the viscoelastic and heterogeneous cell wall fundamentally constrains bacterial growth.

Cell cycle-dependent growth rate—We introduce a minimal model of cell volume growth as a control for the experimental data and define $z \equiv \ln(V/\bar{V}_b)$ where V is the cell volume and $\bar{V}_b$ is the birth volume averaged over cell cycles, which is a constant. In the minimal model, z follows a drifted Brownian motion:

$$dz = kdt + k'dW. \tag{1}$$

Here, t is time, k is the deterministic growth rate, and k' is the noise intensity. dW is a Wiener process where dW is a Gaussian-distributed random number with mean equal to zero and variance equal to dt [16]. Cell division is implemented using the adder model [1, 3, 5]: $V_d(n) = V_b(n) + V_0 + \zeta$ and $V_b(n+1) = V_d(n)/2$. Here, n is the generation number, V_d is the division volume, V_b is the birth volume, V_0 is a constant, and ζ is a Gaussian-distributed random variable. The simulated cell volume

trajectories resemble the experimental ones (Figure 1a, b).

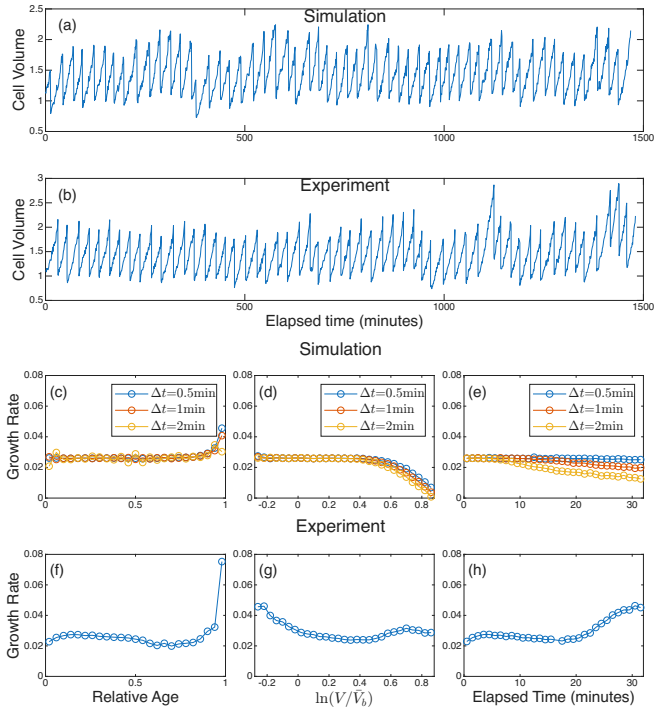

FIG. 1. Cell cycle-dependent growth rate. (a) Cell volume vs. time for the simulation data, where the cell volume is normalized by the average birth volume $\bar{V}_b$. (b) The same as (a) but for the experimental data. (c-e) The growth rate $\lambda = \langle \Delta z / \Delta t \rangle$ averaged over cell cycles for the simulation data vs. relative age (c), $z \equiv \ln(V/\bar{V}_b)$ (d), and the elapsed time (e). (f-h) The same analysis as (c-e) but for the experimental data of *E. coli*. The data is from Ref. [5].

Previous works have shown that the growth rate k was not constant during the cell cycle for *E. coli* and other bacteria [8–10]. To test whether the cell cycle-dependent growth rate is due to real biological processes or data analysis artifacts, we compute the growth rate as $\lambda = \Delta z / \Delta t$ and use approximately the same Δt, about 1 minute for both the experimental and simulation data. Because the growth rate is strictly a constant k in the minimal model, any deviation of the growth rate from k must be a numerical artifact.

We apply three statistical methods to analyze both experimental and simulation data (Figure 1c-h). Surprisingly, all three statistical methods yield systematic biases (Figure 1c-e). In the relative-age statistics, we compute the average growth rate conditioned on a given relative age ϕ during the cell cycle, which is normalized from 0 to 1. Intriguingly, even the simulation data exhibits an apparent acceleration at the end of the cell cycle. In particular, we prove that the average growth rate diverges as $k \sim (1-\phi)^{-1/2}$ near the end of the cell cycle, a pure statistical effect (End Matter).

In contrast, in the relative-volume statistics in which we compute the average growth rate conditioned on a given z, the average growth rate reduces near the end of the cell cycle for the simulation data, and the reduction decreases as Δt decreases (Figure 1d). A similar process occurs in the elapsed-time statistics, where we compute the average growth rate conditioned on a given elapsed time since cell birth (Figure 1e). We leave the discussion of the mechanisms underlying these statistical biases for End Matter, which is not the primary focus of this work.

Given the minimal model as a control, our analysis of experimental data supports the conclusion of super-exponential growth in the second half of the cell cycle, previously proposed in the literature [8–10]. Specifically, for the relative-age statistics, the observed growth-rate acceleration is insufficient to account for the much faster acceleration found in the experimental data (Figure 1f). For the relative-volume and elapsed-time statistics, we still observe a growth-rate acceleration in the second half of the cell cycle (Figure 1g, h), despite the growth-rate reduction predicted from the minimal model.

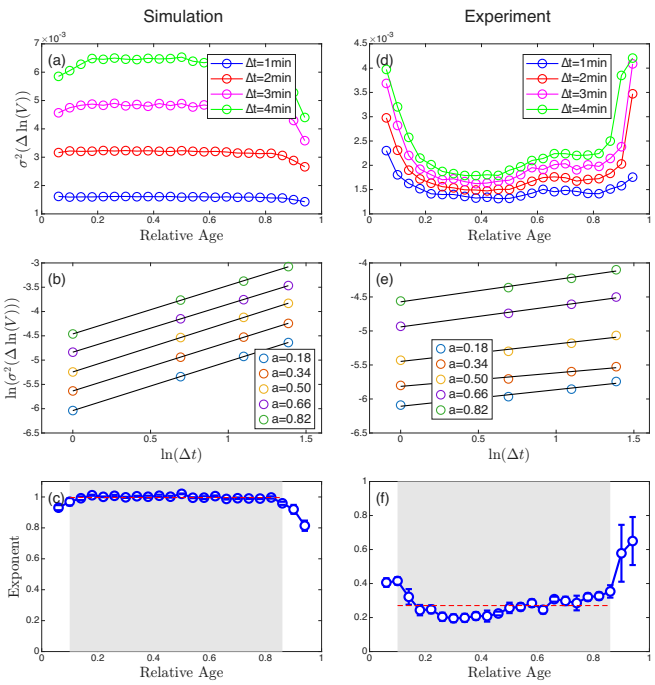

FIG. 2. Subdiffusive random growth of cell volume. (a) $\sigma_z^2(\Delta t)$ vs. the relative age for time intervals $\Delta t = 1, 2, 3$, and 4 min for the simulation data. (b) $\sigma_z^2(\Delta t)$ vs. Δt for several relative ages, from which we calculated the diffusion exponent. Curves for different relative ages are vertically shifted for visual clarity to highlight the robust power-law scaling. (c) The diffusion exponent (α) calculated from the simulation data, plotted against the relative age, showing the reliable regime where α is equal to the ground truth 1. (d-f) The same analysis as (a-c) but for the experimental data. The dashed line in (f) is the average exponent in the reliable regime.

Subdiffusive random growth—Bacterial cell volume is well regulated across cell cycles; however, it is still elu-

sive whether cell volume growth is regulated on a shorter time scale. Therefore, we study fluctuations in cell volume growth using the minimal model as a control. We calculate $\sigma_z^2(\Delta t) = \langle (z(t_0+\Delta t) - z(t_0))^2 \rangle$ given a time interval Δt; here, the average is over cell cycles conditioned on a given relative age, which we call the mean square displacement (MSD) of z in the following. For the minimal model, z is a random walk with a constant drift; therefore, $\sigma_z^2(\Delta t) \sim \Delta t$ (Figure 2a-c). Indeed, the measured exponent was close to one as long as the relative age is not close to zero or one (Figure 2b, c), from which we introduce a regime where the measured exponent is reliable (the shaded area in Figure 2c). Strikingly, we find that the experimental data of z implements a subdiffusive noise (Figure 2d-f):

$$\sigma_z^2(\Delta t) \sim \Delta t^{\alpha}. \tag{2}$$

Notably, the magnitude of the volume fluctuations (σ_z^2) in the experimental data is significantly larger at the early and late stages of the cell cycle (Fig. 2d). This elevated noise level suggests that the complex morphological rearrangements during cell birth and division introduce stronger volume fluctuations compared to the stable elongation phase. However, the α exponent changes mildly throughout the cell cycle, with an average value, $\alpha \approx 0.27$ in the reliable regime. The subdiffusion suggests that the growth rate noise cannot be white noise; instead, the noises at different times must be negatively correlated to generate a subdiffusive MSD of z.

Modeling cell-volume dynamics as a complex viscoelastic material—We remark that the subdiffusion occurs in a time scale of minutes for the experimental data (Figure 2e). Thus, it is unlikely to be generated by biological activities associated with gene expression, which usually takes a doubling time for the protein concentrations to change significantly in bacteria [17]. Therefore, we hypothesize that the subdiffusion comes from a physical process. Considering that cell volume growth always accompanies cell wall growth, and that the cell wall is a complex viscoelastic material [13, 15], we propose that the cell wall mediates the subdiffusive random growth.

We model the cell wall, a peptidoglycan network, as a serial connection of N Voigt elements with elastic and viscous components, which we denote as the general Voigt model (Figure 3a). For one particular Voigt element i, we define its strain as the deviation from its deterministic growth $\Delta\xi_i = \Delta z_i - k_i \Delta t$. For simplicity, we set the growth rate k_i as a constant in the following simulations, which do not affect our conclusions regarding the growth-rate noise. The stress p, which drives cell wall deformation and cell volume growth, corresponds to the turgor pressure (i.e., the difference between cytoplasmic and external osmotic pressures) shared by all elements [18–22]. Here, because we focus on the growth-rate noise, what matters to us is the stress fluctuation,

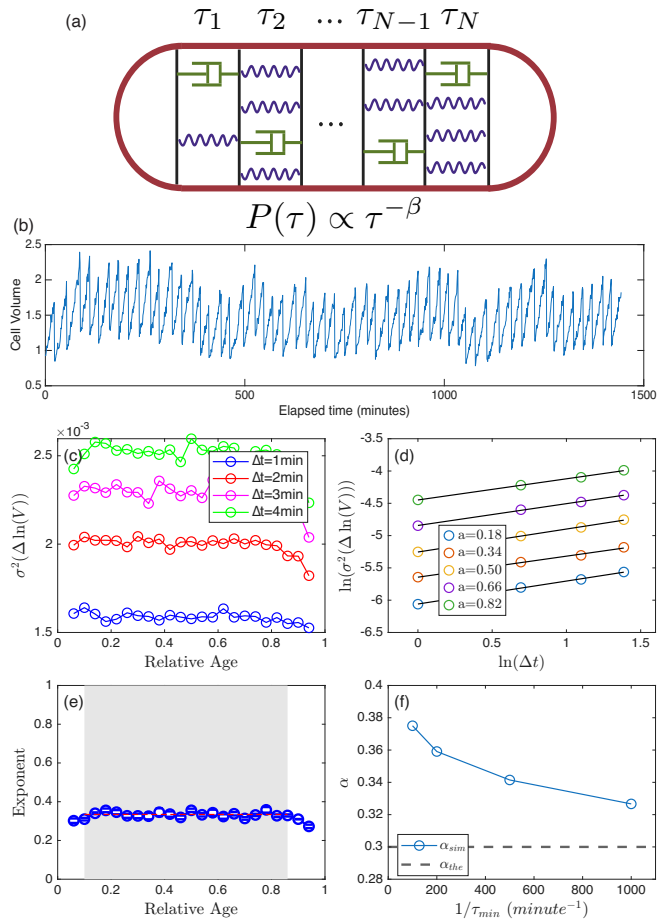

FIG. 3. The general Voigt model of the cell wall recapitulates subdiffusive random growth. (a) We model the cell wall as a serial connection of multiple Voigt elements, each with an elastic component (the spring) and a viscous component (the dashpot). We assume that the relaxation time of each element is random due to the random elastic constant, such that the relaxation time follows a power-law distribution. (b) The same as Figure 1a, but we replace the white noise with the colored noise $\xi(t)$ generated by the general Voigt model in Eq. (1). In the simulations, we set the time unit t_0 as 1 min and the stress unit as η/t_0. We set the dimensionless noise strength $\tilde{A}_p \equiv A_p t_0/\eta^2 \approx 6 \times 10^3$ when $\tau_0 = 0.01$ (Note that A_p is scaled with τ_0 to ensure the growth noise of z remains relatively invariant to the choice of the lower cutoff). (c-e) The same as Figure 2(a-c) but for colored noise. (f) As we decrease the minimum relaxation time τ_0 in the power-law distribution, the measured exponent approaches the predicted value 0.3.

δp, which we set as a white noise, such that $\langle \delta p(t) \rangle = 0$ and $\langle \delta p(t_1) \delta p(t_2) \rangle = 2A_p \delta(t_2 - t_1)$ where A_p is a constant.

Thus, the constitutive equation of each Voigt element becomes

$$\eta \frac{d\xi_i}{dt} = -G_i \xi_i + \delta p, \tag{3}$$

Here, η is the viscosity, and G_i is the elastic modulus of element i. From Eq. (3), we introduce the relaxation

time as $\tau_i = \eta/G_i$, which is random across Voigt elements and follows a power-law distribution (Figure 3a):

$$P(\tau) \sim \tau^{-\beta}, \tag{4}$$

with a lower bound τ_0. In this work, we use "$\sim$" to mean a proportional relationship. We replace the white noise in the minimal model of cell volume growth, Eq. (1) by the colored noise generated by the general Voigt model such that

$$dz(t) = kdt + d\xi(t) \tag{5}$$

where $\xi(t) = \sum_i \xi_i(t)/N$. Solving Eq. (3) for a specific element yields

$$\xi_i(t) \sim \int_{-\infty}^{t} e^{-\frac{t-t'}{\tau_i}} p(t')\mathrm{d}t'. \tag{6}$$

Taking account of the randomly distributed relaxation time, the overall cell growth noise $\xi(t)$ becomes

$$\xi(t) \sim \int_0^{\infty} u^{1-\beta} F(u/\tau_0) p(t-t')\mathrm{d}t', \tag{7}$$

where $F(x) = \int_0^x u^{\beta-2} e^{-u} du$. Given Eq. (7), we find the mean square displacement of $\xi(t)$ as

$$\begin{aligned}\langle[\xi(\Delta t) - \xi(0)]^2\rangle \sim \Delta t^{3-2\beta} \int_0^{\infty} u^{2\beta-4} \Big[F\Big(\frac{\Delta t}{u\tau_0}\Big)^2 \\ - (1+u)^{1-\beta} F\Big(\frac{\Delta t}{u\tau_0}\Big) F\Big(\frac{\Delta t}{u\tau_0} + \frac{\Delta t}{\tau_0}\Big)\Big] du.\end{aligned} \tag{8}$$

Intriguingly, the integral in Eq. (8) approaches a constant in the limit $\Delta t/\tau_0 \gg 1$ given $1 < \beta < 3/2$; consistently, we infer $\beta \approx 1.37$ from the measured α exponent (Figure 2f).

To confirm whether the general Voigt model can recapitulate the experimental phenomena, we simulate the minimal model Eq. (1) with cell cycles included with the noise $\xi(t)$ explicitly generated by N Voigt elements, whose relaxation times are sampled from Eq. (4). We set $\alpha = 0.3$ as the ground truth to test the validity of the theoretical predictions. By averaging ξ_i over all elements, we obtain the time-dependent noise $\xi(t)$ in Eq. (5) (End Matter). Applying the same data analysis protocol as in Figure 2, we find that the minimal model combined with the general Voigt model successfully recapitulates the subdiffusive random growth of bacterial cell volume. In particular, the measured exponent approaches the predicted value $\alpha = 3 - 2\beta$ in the limit of $\Delta t/\tau_0 \to \infty$.

Discussion—In this work, by employing a minimal drifted Brownian motion model as a controlled benchmark, we first identify and correct inherent statistical biases in growth-rate measurements. This analysis confirms that the superexponential acceleration observed in the late cell cycle is a genuine biological feature rather than a sampling artifact.

More importantly, we demonstrate that the stochastic growth of bacterial cell volume exhibits subdiffusive fluctuations, a phenomenon that cannot be accounted for by white-noise growth models. The discovery of subdiffusion, with an anomalous exponent $\alpha \approx 0.27$, suggests that negative temporal correlations govern growth fluctuations. This "memory" in the growth process occurs on timescales significantly shorter than those associated with gene expression or protein synthesis, which typically operate on the scale of a doubling time. Instead, our results point toward a mechanical origin. The success of the general Voigt model, treating the cell wall as a complex viscoelastic network with a power-law distribution of relaxation times $P(\tau) \sim \tau^{-\beta}$ ($\beta \approx 1.37$), suggests that the peptidoglycan meshwork is not merely a plastic shell. Instead, it is a complex material whose multi-scale relaxation dynamics fundamentally constrain the stochastic nature of cell expansion.

The broad distribution of relaxation times implies significant heterogeneity in the cell wall's mechanical properties, potentially stemming from stochastic bond cleavage and glycan strand insertion. Our finding relates the exponent α governing macroscopic growth statistics to the exponent β governing microscopic material parameters. Future work integrating these mechanical fluctuations with the biochemical signaling pathways of cell division may reveal how bacteria harmonize physical constraints with regulatory programs to maintain stable growth.

We remark that the time-averaged growth rate during each cell cycle is constant and the growth rate noise is a white noise in the minimal model, Eq. (1); our conclusions regarding the statistical bias of the average instantaneous growth rate are also valid for more complex models, where the time-averaged growth rate of each cell cycle is random or the noise can have a finite correlation time (Supplemental Material).

Beyond bacterial growth, our study highlights the need for rigorous null models when analyzing biological data. The fact that a minimal model with strictly constant growth rate and Brownian growth-rate noise can exhibit apparent growth acceleration serves as a cautionary note.

We thank Yichen Yan for helpful discussions related to this work. The research was funded by the National Key Research and Development Program of China (2024YFA0919600) and supported by Peking-Tsinghua Center for Life Sciences grants.

* linjie@pku.edu.cn

[1] P.-Y. Ho, J. Lin, and A. Amir, Modeling cell size regulation: From single-cell level statistics to molecular mechanisms and population level effects, arXiv preprint arXiv:1801.00494 (2018).

[2] C. Cadart, L. Venkova, P. Recho, M. C. Lagomarsino,

and M. Piel, The physics of cell-size regulation across timescales, Nature Physics **15**, 993 (2019).
[3] A. Amir, Cell size regulation in bacteria, Physical review letters **112**, 208102 (2014).
[4] M. Campos, I. V. Surovtsev, S. Kato, A. Paintdakhi, B. Beltran, S. E. Ebmeier, and C. Jacobs-Wagner, A constant size extension drives bacterial cell size homeostasis, Cell **159**, 1433 (2014).
[5] S. Taheri-Araghi, S. Bradde, J. T. Sauls, N. S. Hill, P. A. Levin, J. Paulsson, M. Vergassola, and S. Jun, Cell-size control and homeostasis in bacteria, Current Biology **25**, 385 (2015).
[6] P. Wang, L. Robert, J. Pelletier, W. L. Dang, F. Taddei, A. Wright, and S. Jun, Robust growth of escherichia coli, Current Biology **20**, 1099 (2010).
[7] M. Godin, F. F. Delgado, S. Son, W. H. Grover, A. K. Bryan, A. Tzur, P. Jorgensen, K. Payer, A. D. Grossman, M. W. Kirschner, *et al.*, Using buoyant mass to measure the growth of single cells, Nature methods **7**, 387 (2010).
[8] P. Kar, S. Tiruvadi-Krishnan, J. Männik, J. Männik, and A. Amir, Distinguishing different modes of growth using single-cell data, eLife **10**, e72565 (2021).
[9] A. Cylke and S. Banerjee, Super-exponential growth and stochastic size dynamics in rod-like bacteria, Biophysical Journal **122**, 1254 (2023).
[10] A. Cylke and S. Banerjee, Gene expression cycles drive non-exponential bacterial growth, Phys. Rev. Res. **7**, 033123 (2025).
[11] G. Seltmann and O. Holst, *The bacterial cell wall* (Springer Science & Business Media, 2002).
[12] S. O. Meroueh, K. Z. Bencze, D. Hesek, M. Lee, J. F. Fisher, T. L. Stemmler, and S. Mobashery, Three-dimensional structure of the bacterial cell wall peptidoglycan, Proceedings of the National Academy of Sciences **103**, 4404 (2006).
[13] V. Vadillo-Rodriguez, T. J. Beveridge, and J. R. Dutcher, Surface viscoelasticity of individual gram-negative bacterial cells measured using atomic force microscopy, Journal of Bacteriology **190**, 4225 (2008).
[14] G. K. Auer and D. B. Weibel, Bacterial cell mechanics, Biochemistry **56**, 3710 (2017).
[15] A. Weber, D. Tyrakowski, and J. L. Toca-Herrera, Power laws describe bacterial viscoelasticity, Langmuir **38**, 15552 (2022).
[16] C. W. Gardiner, *Handbook of Stochastic Methods: for Physics, Chemistry and the Natural Sciences*, 3rd ed., Vol. 13 (Springer, Berlin, 2004).
[17] R. Milo and R. Phillips, *Cell biology by the numbers* (Garland Science, 2015).
[18] M. Arnoldi, M. Fritz, E. Bäuerlein, M. Radmacher, E. Sackmann, and A. Boulbitch, Bacterial turgor pressure can be measured by atomic force microscopy, Phys. Rev. E **62**, 1034 (2000).
[19] Y. Deng, M. Sun, and J. W. Shaevitz, Direct measurement of cell wall stress stiffening and turgor pressure in live bacterial cells, Physical Review Letters **107**, 158101 (2011).
[20] E. Rojas, J. A. Theriot, and K. C. Huang, Response of escherichia coli growth rate to osmotic shock, Proceedings of the National Academy of Sciences **111**, 7807 (2014).
[21] H. Zhang, H. Wang, J. J. Wilksch, R. A. Strugnell, M. L. Gee, and X.-Q. Feng, Measurement of the interconnected turgor pressure and envelope elasticity of live bacterial cells, Soft Matter **17**, 2042 (2021).
[22] Y. Ye, Q. Wang, and J. Lin, Physical constraints and biological regulations underlie universal osmoresponses, eLife **13**, RP102858 (2025).

End Matter

Details of numerical simulations

We perform numerical simulations of the stochastic growth dynamics using a multi-scale integration scheme. The stochastic differential equation (SDE) for cell volume growth [Eq. (1)] is integrated with a time step of $\delta t = 0.05$ min. To match the 1-min sampling interval of the experimental data [5], the simulation trajectories were sampled every 20th data point. The division process follows the adder model, with noise magnitudes in both the SDE and the division volume tuned to recapitulate the observed volume trajectories in experiments.

For the viscoelastic growth model (Figure 3), we generate the colored noise $\xi(t)$ by simulating $N = 10000$ Voigt elements with a higher resolution time step of 0.001 min for the case of $\tau_0 = 0.01$ (N is also scaled with τ_0 to maintain a constant expectation for the maximum τ). Each integration step of the growth SDE thus incorporated the cumulative strain over 50 internal steps of the Voigt dynamics. To ensure the colored noise statistics reach a stationary state, we implement a "pre-warming" period for each lineage in which the Voigt model is equilibrated for 10 min from a zero-strain initial state before being coupled to the volume SDE. We note that the growth rate noise $\xi(t)$ is generated independently for each simulated lineage.

Mechanisms of the statistical biases in the cell cycle-dependent growth rate

Near the end of the cell cycle, for those cells that are about to reach the division size, their instantaneous growth rates are dominated by the random term in Equation 1, that is, $\lambda \sim (1-\phi)^{-1/2}$, giving rise to the divergence of the average growth rate conditioned on the relative age. According to this argument, the growth-rate divergence should be invariant of Δt, which we confirmed numerically (Figure 1c). We remark that a similar result should hold for colored noise, e.g., the noise generated by the general Voigt model. If the mean-square-displacement (MSD) of the growth rate noise follows $\sigma_z^2(\Delta t)\rangle \sim \Delta t^{\alpha}$, we expect that $\lambda \sim (1-\phi)^{\alpha/2-1}$ near the end of the cell cycle. We include a more detailed analytical derivation for the Brownian case in the Supplemental Material.

For the relative-volume statistics, the reduction of the growth rate near the end of the cell cycle is because a cell whose instantaneous growth rate is high at the end

of the cell cycle can miss the last $\ln(V/\bar{V}_b)$ bin in its cell-volume trajectory. Therefore, the average growth rate is biased toward cells with slower instantaneous growth rates. Thus, we predict that the growth-rate reduction should decrease as Δt decreases, which we confirmed numerically (Figure 1g). A similar process occurs in the elapsed-time statistics, where we compute the average growth rate conditioned on a given elapsed time since cell birth (Figure 1h).